A NEWTON-EULER FORMULATION FOR THE INVERSE DYNAMICS OF THE STEWART PLATFORM MANIPULATOR

BHASKAR DASGUPTA† and T. S. MRUTHYUNJAYA

Department of Mechanical Engineering, Indian Institute of Science, Bangalore—560 012, India

Abstract—This paper presents an inverse dynamic formulation by the Newton–Euler approach for the Stewart platform manipulator of the most general architecture and models all the dynamic and gravity effects as well as the viscous friction at the joints. It is shown that a proper elimination procedure results in a remarkably economical and fast algorithm for the solution of actuator forces, which makes the method quite suitable for on-line control purposes. In addition, the parallelism inherent in the manipulator and in the modelling makes the algorithm quite efficient in a parallel computing environment, where it can be made as fast as the corresponding formulation for the 6-dof serial manipulator. The formulation has been implemented in a program and has been used for a few trajectories planned for a test manipulator. Results of simulation presented in the paper reveal the nature of the variation of actuator forces in the Stewart platform and justify the dynamic modelling for control. © 1998 Elsevier Science Ltd. All rights reserved

1. INTRODUCTION

In contrast to the open-chain serial manipulators, the dynamic modelling of parallel manipulators presents an inherent complexity due to their closed-loop structure and kinematic constraints. Nevertheless, the dynamic modelling is quite important for their control, particularly because parallel manipulators are preferred in applications where precise positioning and good dynamic performance under high load are the prime requirements. In recent years, there has been a great amount of research on the kinematics of parallel manipulators, but works on the dynamics of parallel manipulators are relatively few. The present work deals with the dynamic formulation of the Stewart platform, which is the most celebrated parallel manipulator.

The Stewart platform is a six-degree-of-freedom mechanism with two bodies connected together by six extensible legs. This manipulating structure is obtained from generalization of the mechanism originally proposed by Stewart[1] as a flight simulator. The general Stewart platform has a base and a platform connected by six extensible legs‡ with spherical joints at both ends or spherical joint at one end and universal joint at the other. In the present work, the kinematic structure with universal joints at the base and spherical joints at the platform has been considered.

The static force analysis of the Stewart platform[2] is straightforward and it is easy to find the leg forces required to support a given force and moment acting on the platform. By slight extension of this force transformation, Fichter[3] incorporated the gravity and dynamic forces on the platform and formulated the inverse dynamics of Stewart platform with massless legs and frictionless joints.

Do and Yang[4] solved the inverse dynamics of the Stewart platform by Newton–Euler method assuming the joints as frictionless and legs as symmetrical and thin (i.e. the centre of gravity of a leg lies on its axis and axial moment of inertia is negligible). They presented some simulation results for tracking certain trajectories and found the required forces for various manipulator parameters. In their work, the rotational equilibrium of the two parts of each leg is considered together with variable moment of inertia, but in the algorithm for path tracking, the moment of inertia of the leg has not been updated as a function of configuration.

---

†Now at Department of Mechanical Engineering, Indian Institute of Technology, Kanpur-208 016, India; e-mail: dasgupta@ütk.ernet.in; tel: 0091-512-597095/597995; fax: 0091-512-597995.
‡Each leg is a system of two bodies connected by a prismatic actuation giving the variable length.

Geng *et al.* [5] developed the Lagrangian equations of motion for the Stewart platform with the platform position and orientation variables as generalised coordinates. Liu *et al.* [6] developed a similar system of dynamic equations and derived the dynamic equations for control by transforming the equations to joint space. Ji [7] considered the question of leg inertia and studied its effect on the dynamics of the Stewart platform.

In the present work, the inverse dynamics of the Stewart platform has been formulated by Newton–Euler approach and unwanted force components have been eliminated to arrive at a system of six linear equations in six unknowns from which the required input forces at the legs can be obtained directly. If the constraint forces are also required, as for the mechanical design, they can be determined by a small amount of additional computation.

The mechanism modelled has a universal joint† at the base end and a spherical joint at the platform end of each leg (see Fig. 1). The disposition of base points and platform points, the directions of the fixed axes at the base and the mass distribution of the legs are completely arbitrary, and no assumption has been made concerning the kinematic and dynamic parameters of the manipulator. The formulation incorporates all the dynamic (inertia, centripetal, coriolis), gravity and external forces, and includes the viscous friction at the joints. It is assumed that the links are rigid. Coulomb friction at the joints has been neglected. The inertia of the universal joints, being negligible, has not been considered in the formulation.

Though the present formulation deals with universal joints at the base, it is applicable to the similar mechanism with spherical joints at both ends as well. The only difference will be that the axial rotation of the legs will be allowed in that case, and certain symmetry assumptions about the dynamic parameters of the legs have to be made as there is no way to control the passive freedom of the legs.

The next section described the kinematics and dynamics of the legs and identifies the contribution of each leg to the force system acting on the platform. Section 3 deals with the kinematics and dynamics of the platform and solution of the required leg forces and the constraint forces also (if necessary). Section 4 develops the framework used for implementing the algorithm and Section 5 presents some results concerning the nature of leg forces required to track a few planned trajectories. Finally, in the last section, the conclusions of the present work and the further issues that it raises have been discussed.

The following notations have been used in this paper.

$$\mathbf{t} = \text{translation vector (position of platform)}$$
$$\Re = \text{rotation matrix (orientation of platform)}$$
$$\dot{\mathbf{t}} = \text{linear velocity of reference point of platform}$$
$$\omega = \text{angular velocity of platform}$$
$$\ddot{\mathbf{t}} = \text{linear acceleration of reference point of platform}$$
$$\alpha = \text{angular acceleration of platform}$$
$$M = \text{mass of platform}$$
$$\mathbf{R}_0 = \text{centre of gravity of platform (in platform frame)}$$
$$\mathbf{I}_p = \text{moment of inertia of platform (in platform frame)}$$
$$\mathbf{F}_{ext} = \text{external force on the platform (in platform frame)}$$
$$\mathbf{M}_{ext} = \text{external moment on the platform (in platform frame)}$$
$$\mathbf{b}_i = i\text{th base point}$$
$$\mathbf{k}_i = \text{stationary axis of the universal joint at } i\text{th leg}$$
$$\mathbf{p_i} = i\text{th platform point (in platform frame)}$$
$$\mathbf{q_i} = \Re \mathbf{p_i}$$
$$\mathbf{T}_i = \text{rotation matrix giving orientation of } i\text{th leg}$$
$$(m_d)_i, (m_u)_i = \text{masses of lower and upper part of } i\text{th leg}$$
$$(\mathbf{r}_{d0})_i, (\mathbf{r}_{u0})_i = \text{CG of lower and upper part of } i\text{th leg (in local frames)}$$
$$(\mathbf{I}_{d0})_i, (\mathbf{I}_{u0})_i = \text{moments of inertia of lower and upper part of } i\text{th leg (in local frame)}$$
$$\mathbf{g} = \text{acceleration due to gravity}$$
$$C_u, C_p, C_s = \text{coefficients of viscous friction in the universal, prismatic and spherical joints,}$$
$$\text{respectively}$$
$$F_i = \text{input force required at } i\text{th leg.}$$

---

†It has two degrees-of-freedom of rotation about two perpendicular axes and is constrained against rotation about the leg axis.
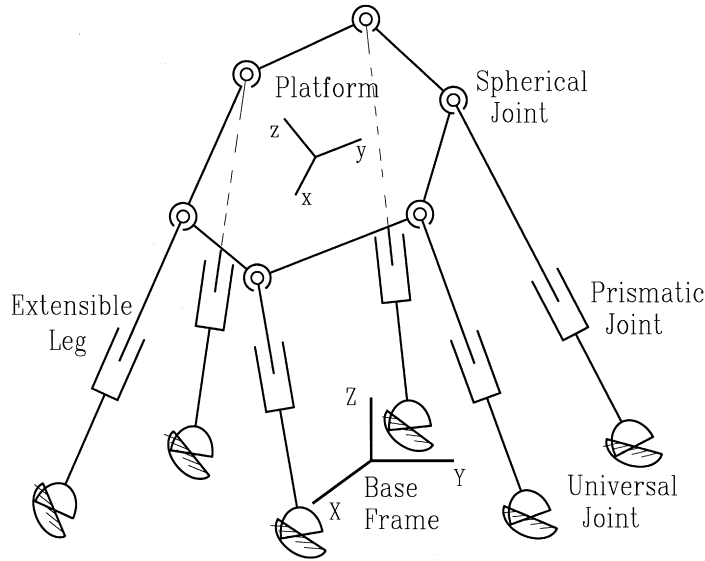
Fig. 1. The Stewart platform.

Other symbols have been described at the place of first occurrence. In general, boldface symbols have been used for vectors and matrices. Leg numbers have been denoted by subscripts.

2. KINEMATICS AND DYNAMICS OF A LEG

This section describes the kinematics and dynamics of a single leg and expresses the contribution of each leg to the force system acting on the platform in terms of one unknown by eliminating the others. Throughout the section, all variables except the kinematic variables of the platform, i.e. position, velocity and acceleration, pertain to an arbitrary leg. So, the leg index i has been dropped from the equations for convenience and it is understood that the equations are applicable to any leg in general.

2.1 Kinematics of a leg

One leg of the manipulator has been shown in Fig. 2 with the associated symbols. Apart from the fixed base frame and the mobile platform frame (shown as frame $\mathbf{P}$), two other frames of reference, namely frame $\mathbf{D}$ and frame $\mathbf{U}$, have been shown which are attached to the lower and upper parts of the legs.

The platform connection point $\mathbf{p}$ (as expressed in the platform frame) can be transformed to base frame by the use of the platform translation $\mathbf{t}$ and rotation $\Re$ relative to the base as

$$(\mathbf{p})_{\text{Base}} = \Re\mathbf{p} + \mathbf{t}.$$

Then, the leg vector $\mathbf{S}$ (vector from the origin of the frame $\mathbf{D}$ to the origin of the frame $\mathbf{U}$) can be found from the difference of the position vectors of the platform point and the base point. Thus, we obtain

$$\mathbf{S} = \Re\mathbf{p} + \mathbf{t} - \mathbf{b}$$

or

$$\mathbf{S} = \mathbf{q} + \mathbf{t} - \mathbf{b} \tag{1}$$

which is the inverse kinematic equation for the Stewart platform.

The leg length and the unit vector along the leg are given by

$$L = \|\mathbf{S}\| \tag{2}$$

and

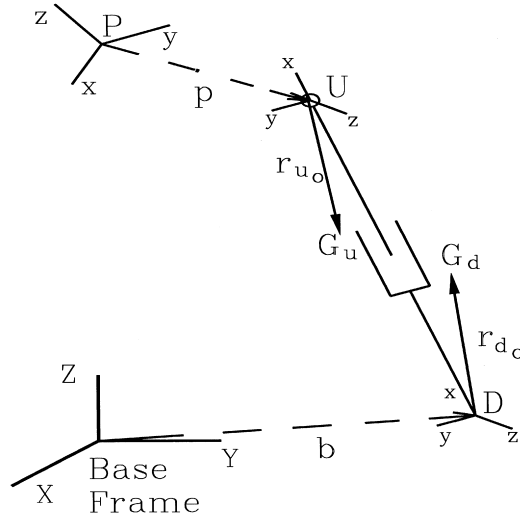$$\mathbf{s} = \mathbf{S}/\mathbf{L}. \tag{3}$$

Fig. 2. Details of one leg.

The velocity of the platform-connection-point of the leg is the time derivative of the leg vector and is given in terms of the platform velocities as

$$\dot{\mathbf{S}} = \boldsymbol{\omega} \times \mathbf{q} + \dot{\mathbf{t}}. \tag{4}$$

The sliding velocity between the two parts of the leg is given by the component of this velocity along the leg.

$$\dot{L} = \mathbf{s} \cdot \dot{\mathbf{S}}. \tag{5}$$

The component of $\dot{\mathbf{S}}$ perpendicular to the leg is related to the angular velocity $\mathbf{W}$ of the leg as

$$\mathbf{W} \times \mathbf{S} = \dot{\mathbf{S}} - \dot{L}\mathbf{s}.$$

Taking the cross product of the above equation with $\mathbf{s}$ and observing that no rotation is allowed about the leg axis (i.e. $\mathbf{s} \cdot \mathbf{W} = 0$), we obtain

$$\mathbf{W} = \mathbf{s} \times \dot{\mathbf{S}}/L. \tag{6}$$

Again, the acceleration of the platform-connection-point is the time derivative of the velocity and is expressed in terms of the linear and angular accelerations of the platform as

$$\ddot{\mathbf{S}} = \boldsymbol{\alpha} \times \mathbf{q} + \boldsymbol{\omega} \times (\boldsymbol{\omega} \times \mathbf{q}) + \ddot{\mathbf{t}}. \tag{7}$$

This acceleration can be expressed in terms of the sliding acceleration $\ddot{L}$ at the prismatic joint and the angular acceleration $\mathbf{A}$ of the leg as

$$\ddot{\mathbf{S}} = \ddot{L}\mathbf{s} + \mathbf{W} \times (\mathbf{W} \times \mathbf{S}) + 2\mathbf{W} \times \dot{L}\mathbf{s} + \mathbf{A} \times \mathbf{S}.$$

Simplifying and using $\mathbf{s} \cdot \mathbf{W} = 0$, we obtain

$$\ddot{\mathbf{S}} = (\ddot{L} - L\mathbf{W} \cdot \mathbf{W})\mathbf{s} + 2\mathbf{W} \times \dot{L}\mathbf{s} + \mathbf{A} \times \mathbf{S}.$$

Now, taking the component along the leg by the dot product with $\mathbf{s}$, the sliding acceleration between the two parts of the leg is given by

$$\ddot{L} = \mathbf{s} \cdot \ddot{\mathbf{S}} + L\mathbf{W} \cdot \mathbf{W}. \tag{8}$$

Similarly, taking the cross product of the same equation with $\mathbf{s}$ and using the fact that no axial rotation of the leg is allowed (i.e. $\mathbf{s} \cdot \mathbf{W} = 0$ and $\mathbf{s} \cdot \mathbf{A} = 0$), we obtain the angular acceleration of the leg as

$$\mathbf{A} = (\mathbf{s} \times \ddot{\mathbf{S}} - 2\dot{L}\mathbf{W})/L. \tag{9}$$

The above expressions determine the position, velocity and acceleration of the leg. Here, use has been made of the fact that no axial rotation of the leg is allowed by the universal joint. In the case of spherical joints at both the ends of the leg, this condition is not there, but the velocity and acceleration components associated with axial rotation can be ignored as they are not controllable.

2.2 Leg acceleration and inertia

A frame of reference (shown as frame **D** in Fig. 2) is attached to the lower part of the leg with its origin at the base-point, x-axis along the leg, y-axis along the rotating axis (axis fixed to the leg) of the universal joint and z-axis perpendicular to the x and y axes according to the right hand rule. Another frame of reference (frame **U** in Fig. 2) with the same orientation is attached to the upper part of the leg with the origin at the platform-point. The kinematic and dynamic parameters of the leg have to be transformed to a fixed frame (not shown separately in the figure) of reference parallel to the base frame at the base-point.

The transformation from the moving lower frame to the fixed leg frame is just a rotation. The x, y and z axes of the moving lower frame are

$$
\begin{aligned}
x\text{-axis} \quad & \hat{\mathbf{x}} = \mathbf{s} \\
y\text{-axis} \quad & \hat{\mathbf{y}} = (\mathbf{k} \times \mathbf{s})/\|\mathbf{k} \times \mathbf{s}\| \, . \\
z\text{-axis} \quad & \hat{\mathbf{z}} = \hat{\mathbf{x}} \times \hat{\mathbf{y}}
\end{aligned}
$$

Hence the transformation matrix is

$$\mathbf{T} = [\hat{\mathbf{x}}\,\hat{\mathbf{y}}\,\hat{\mathbf{z}}]. \tag{10}$$

The transformation from the moving upper frame to fixed leg frame is the same rotation matrix along with the translation equal to the leg vector.

If $\mathbf{r}_{d_0}$ and $\mathbf{r}_{u_0}$ denote the position vectors of the centres of gravity (G_l and G_u, respectively) of the lower and the upper parts in their respective frames of reference, then they can be transformed to the fixed leg frame as

$$\mathbf{r}_d = \mathbf{T}\mathbf{r}_{d_0} \tag{11}$$

$$\mathbf{r}_u = \mathbf{T}(\mathbf{v} + \mathbf{r}_{u_0}) \tag{12}$$

where

$$\mathbf{v} = [L\,0\,0]^{\mathrm{T}}.$$

The acceleration of the centres of gravity of the two parts are then

$$\mathbf{a}_d = \mathbf{A} \times \mathbf{r}_d + \mathbf{W} \times (\mathbf{W} \times \mathbf{r}_d) \tag{13}$$

$$\mathbf{a}_u = \ddot{L}\mathbf{s} + \mathbf{A} \times \mathbf{r}_u + \mathbf{W} \times (\mathbf{W} \times \mathbf{r}_u) + 2\dot{L}\mathbf{W} \times \mathbf{s}. \tag{14}$$

The moment of inertia $\mathbf{I}_d$ of the lower part in the fixed leg frame can be obtained from its moment of inertia $\mathbf{I}_{d_0}$ in its local frame by the rotation transformation

$$\mathbf{I}_d = \mathbf{T}\mathbf{I}_{d_0}\mathbf{T}^{\mathrm{T}}. \tag{15}$$

The transformation of the moment of inertia of the upper part involves a rotation as well as a translation.

$$\mathbf{I}_u = \mathbf{T}[\mathbf{I}_{u_0} + m_u L^2 \mathrm{diag}(0,\,1,\,1)]\mathbf{T}^{\mathrm{T}} \tag{16}$$

where

$$\text{diag}(0, 1, 1) = \begin{bmatrix} 0 & 0 & 0 \\ 0 & 1 & 0 \\ 0 & 0 & 1 \end{bmatrix}$$

because the theorem of parallel axes gives the transformation of moment of inertia by a displacement of "$\mathbf{v}$" as $\mathbf{I}_0 + m(\mathbf{v}^T\mathbf{v}\mathbf{E}_3 - \mathbf{v}\mathbf{v}^T)$ and here

$$\mathbf{v}^T\mathbf{v}\mathbf{E}_3 - \mathbf{v}\mathbf{v}^T = L^2\text{diag}(0, 1, 1)$$

where $\mathbf{E}_3$ is the 3×3 identity matrix.

2.3 Dynamic equations for a leg

The equations of motion for each leg will give 12 equations (three force equations and three moment equations for each of the lower and upper parts of the leg) in the 13 unknowns (six unknown forces and moments at the prismatic joint, three forces and one moment at the universal joint and three forces at the spherical joint) for each leg. As there is one unknown in excess of the number of equations for each leg, all the unknowns can be expressed in terms of only one unknown for each leg. A judicious ordering of the equations has been used here to facilitate the elimination of the constraint forces from the equations so that the unknown force from the leg to the platform required to derive the equations of motion for the platform can be expressed in terms of only one unknown.

Considering the moments acting on the lower part of the leg in the fixed leg frame, Euler's equation gives

$$-m_d\mathbf{r}_d \times \mathbf{a}_d + m_d\mathbf{r}_d \times \mathbf{g} - \mathbf{I}_d\mathbf{A} - \mathbf{W} \times \mathbf{I}_d\mathbf{W} + M_u\mathbf{s} - \mathbf{r} \times \mathbf{F}_p - \mathbf{M}_p - C_u\mathbf{W} = 0 \qquad (17)$$

where M_u is the magnitude of the constraint moment at the universal joint acting about the leg axis, $\mathbf{F}_p$ is the vector force at the prismatic joint exerted by the lower part on the upper part acting at a point $\mathbf{r}$, $\mathbf{M}_p$ is the vector moment at the prismatic joint acting on the upper part and the last term in the equation is the moment of viscous friction at the universal joint.

Similarly, Euler's equation for the upper part of the leg gives

$$-m_u\mathbf{r}_u \times \mathbf{a}_u + m_u\mathbf{r}_u \times \mathbf{g} - \mathbf{I}_u\mathbf{A} - \mathbf{W} \times \mathbf{I}_u\mathbf{W} + \mathbf{S} \times \mathbf{F}_s + \mathbf{r} \times \mathbf{F}_p + \mathbf{M}_p - \mathbf{f} = 0 \qquad (18)$$

where

$$\mathbf{f} = C_s(\mathbf{W} - \boldsymbol{\omega})$$

is the moment of viscous friction at the spherical joint and $\mathbf{F}_s$ is the constraint force at the spherical joint acting on the leg.

Adding Equations (17) and (18), we obtain Euler's equation for the complete leg as

$$-m_d\mathbf{r}_d \times \mathbf{a}_d - m_u\mathbf{r}_u \times \mathbf{a}_u + (m_d\mathbf{r}_d + m_u\mathbf{r}_u) \times \mathbf{g} - (\mathbf{I}_d + \mathbf{I}_u)\mathbf{A}$$
$$-\mathbf{W} \times (\mathbf{I}_d + \mathbf{I}_u)\mathbf{W} + M_u\mathbf{s} + \mathbf{S} \times \mathbf{F}_s - C_u\mathbf{W} - \mathbf{f} = 0 \qquad (19)$$

or,

$$M_u\mathbf{s} + \mathbf{S} \times \mathbf{F}_s = \mathbf{C} \qquad (20)$$

where

$$\mathbf{C} = m_d\mathbf{r}_d \times \mathbf{a}_d + m_u\mathbf{r}_u \times \mathbf{a}_u - (m_d\mathbf{r}_d + m_u\mathbf{r}_u) \times \mathbf{g} + (\mathbf{I}_d + \mathbf{I}_u)\mathbf{A} + \mathbf{W} \times (\mathbf{I}_d + \mathbf{I}_u)\mathbf{W} + C_u\mathbf{W} + \mathbf{f}.$$

The scalar unknown M_u can be eliminated from Equation (20) by taking cross products of both sides with $\mathbf{s}$ as

$$\mathbf{s} \times (\mathbf{S} \times \mathbf{F}_s) = \mathbf{s} \times \mathbf{C}$$

or,

$$\mathbf{F}_s = x\mathbf{s} + \frac{\mathbf{C} \times \mathbf{s}}{L} = x\mathbf{s} + \mathbf{K} \qquad (21)$$

where

$$x = \mathbf{s} \cdot \mathbf{F}_{\mathrm{s}} \tag{22}$$

is the component of the force $\mathbf{F}_{\mathrm{s}}$ at the spherical joint along the leg and

$$\mathbf{K} = \frac{\mathbf{C} \times \mathbf{s}}{L}$$

is a known vector.

Equation (21) expresses the force $\mathbf{F}_{\mathrm{s}}$ in terms of a single unknown x for the leg and this force is the contribution of the leg to the force system acting on the platform.

Finally, we consider the upper part of the leg and Newton's equation gives

$$-m_{\mathrm{u}}\mathbf{a}_{\mathrm{u}} + m_{\mathrm{u}}\mathbf{g} + \mathbf{F}_{\mathrm{p}} + \mathbf{F}_{\mathrm{s}} - C_{\mathrm{p}}\dot{L}\mathbf{s} = 0 \tag{23}$$

in which the last term is the viscous resistance at the prismatic joint.

As we are interested in the axial component of $\mathbf{F}_{\mathrm{p}}$ which is the actuating force, we can take the component of the above equation in the direction of the leg by taking the dot product with $\mathbf{s}$ obtaining

$$\mathbf{s} \cdot \mathbf{F}_{\mathrm{p}} = m_{\mathrm{u}}\mathbf{s} \cdot (\mathbf{a}_{\mathrm{u}} - \mathbf{g}) + C_{\mathrm{p}}\dot{L} - \mathbf{s} \cdot \mathbf{F}_{\mathrm{s}}.$$

Substituting from Equation (22) in the above, we obtain

$$F = D - x \tag{24}$$

where F is the actuator force and

$$D = m_{\mathrm{u}}\mathbf{s} \cdot (\mathbf{a}_{\mathrm{u}} - \mathbf{g}) + C_{\mathrm{p}}\dot{L}.$$

Equation (24) gives the actuator force in terms of the unknown x for the leg. The unknown x for the ith leg can be denoted by x_i and the six unknowns for the six legs have to be solved from the equations of motion for the platform, which are derived in the next section. So far as the computation of the actuator forces are concerned, there is no necessity of considering Newton's equations for the lower part of the leg because those equations will involve an equal number of unknown constraint forces at the universal joints. However, for the determination of the reaction at the universal joint, Newton's equation for the lower part of the leg can be written as

$$-m_{\mathrm{d}}\mathbf{a}_{\mathrm{d}} + m_{\mathrm{d}}\mathbf{g} - \mathbf{F}_{\mathrm{p}} + \mathbf{F}_{\mathrm{u}} + C_{\mathrm{p}}\dot{L}\mathbf{s} = 0$$

or,

$$\mathbf{F}_{\mathrm{u}} = m_{\mathrm{d}}(\mathbf{a}_{\mathrm{d}} - \mathbf{g}) + \mathbf{F}_{\mathrm{p}} - C_{\mathrm{p}}\dot{L}\mathbf{s} \tag{25}$$

where $\mathbf{F}_{\mathrm{p}}$ can be solved from Equation (23) as

$$\mathbf{F}_{\mathrm{p}} = m_{\mathrm{u}}(\mathbf{a}_{\mathrm{u}} - \mathbf{g}) - \mathbf{F}_{\mathrm{s}} + C_{\mathrm{p}}\dot{L}\mathbf{s}. \tag{26}$$

Consequently,

$$F_{\mathrm{u}} = m_{\mathrm{d}}\mathbf{a}_{\mathrm{d}} + m_{\mathrm{u}}\mathbf{a}_{\mathrm{u}} - (m_{\mathrm{d}} + m_{\mathrm{u}})\mathbf{g} - \mathbf{F}_{\mathrm{s}}. \tag{27}$$

The constraint force $\mathbf{F}_c$ at the prismatic joint can be determined from

$$\mathbf{F}_c = \mathbf{F}_p - \mathbf{s}F. \tag{28}$$

The magnitude M_u of the constraint moment at the universal joint can be obtained from Equation (20) as

$$M_u = \mathbf{s} \cdot \mathbf{C}. \tag{29}$$

3. KINEMATICS AND DYNAMICS OF THE PLATFORM

In the preceding section, the reaction force $(\mathbf{F}_s)_i$ at the ith spherical joint was expressed in terms of the unknown x_i. In this section, the equations of motion for the platform will be developed as six linear equations in those six unknowns pertaining to the six legs.

3.1 Acceleration and inertia of the platform

If $\mathbf{R}_0$ be the position vector of the centre of gravity of the platform (including the payload) in the local frame of reference, the same vector expressed in the base frame will be

$$\mathbf{R} = \Re\mathbf{R}_0. \tag{30}$$

Therefore, the acceleration of the centre of gravity is

$$\mathbf{a} = \boldsymbol{\alpha} \times \mathbf{R} + \boldsymbol{\omega} \times (\boldsymbol{\omega} \times \mathbf{R}) + \ddot{\mathbf{t}}. \tag{31}$$

The moment of inertia $\mathbf{I}_p$ of the platform (including the payload) can be transformed to the global basis as

$$\mathbf{I} = \Re\mathbf{I}_p\Re^T. \tag{32}$$

3.2 Dynamic equations for the platform

It is assumed that external force system (if any) acting on the platform is available as a force $\mathbf{F}_{ext}$ and a moment $\mathbf{M}_{ext}$ in the local frame of reference. These vectors can be transformed to the global basis by the rotation transformation.

Hence, Newton's equation for the platform can be written as

$$-M\mathbf{a} + M\mathbf{g} + \Re\mathbf{F}_{ext} - \sum_{i=1}^{6}(\mathbf{F}_s)_i = 0.$$

Substituting the expression for $(\mathbf{F}_s)_i$ from Equation (21), we obtain

$$\sum_{i=1}^{6} x_i\mathbf{s}_i = \Re\mathbf{F}_{ext} + M(\mathbf{g} - \mathbf{a}) + \sum_{i=1}^{6} \mathbf{K}_i. \tag{33}$$

Taking the moments about the platform reference point, Euler's equation for the platform gives

$$-M\mathbf{R} \times \mathbf{a} + M\mathbf{R} \times \mathbf{g} - \mathbf{I}\boldsymbol{\alpha} - \boldsymbol{\omega} \times \mathbf{I}\boldsymbol{\omega} + \Re\mathbf{M}_{ext} - \sum_{i=1}^{6}[\mathbf{q}_i \times (\mathbf{F}_s)_i] + \sum_{i=1}^{6} \mathbf{f}_i = 0.$$

Again, substituting from Equation (21) results in

$$\sum_{i=1}^{6}[x_i\mathbf{q}_i \times \mathbf{s}_i] = M\mathbf{R} \times (\mathbf{g} - \mathbf{a}) - \mathbf{I}\boldsymbol{\alpha} - \boldsymbol{\omega} \times \mathbf{I}\boldsymbol{\omega} + \Re\mathbf{M}_{ext} - \sum_{i=1}^{6}[\mathbf{q}_i \times \mathbf{K}_i - \mathbf{f}_i]. \tag{34}$$

Equations (33) and (34) give six equations in the six unknowns $x_1, x_2, \ldots, x_6$. Combining them, the complete equation is

$$\begin{bmatrix} \mathbf{s}_1 & \mathbf{s}_2 & \mathbf{s}_3 & \mathbf{s}_4 & \mathbf{s}_5 & \mathbf{s}_6 \\ \mathbf{q}_1 \times \mathbf{s}_1 & \mathbf{q}_2 \times \mathbf{s}_2 & \mathbf{q}_3 \times \mathbf{s}_3 & \mathbf{q}_4 \times \mathbf{s}_4 & \mathbf{q}_5 \times \mathbf{s}_5 & \mathbf{q}_6 \times \mathbf{s}_6 \end{bmatrix} \begin{bmatrix} x_1 \\ x_2 \\ x_3 \\ x_4 \\ x_5 \\ x_6 \end{bmatrix}$$

$$= \begin{bmatrix} \Re\mathbf{F}_{\text{ext}} + M(\mathbf{g} - \mathbf{a}) - \sum_{i=1}^{6} \mathbf{K}_i \\ M\mathbf{R} \times (\mathbf{g} - \mathbf{a}) - \mathbf{I}\boldsymbol{\alpha} - \boldsymbol{\omega} \times \mathbf{I}\boldsymbol{\omega} + \Re\mathbf{M}_{\text{ext}} - \sum_{i=1}^{6}[\mathbf{q}_i \times \mathbf{K}_i - \mathbf{f}_i] \end{bmatrix} \quad (35)$$

or,

$$\mathbf{Hx} = \mathbf{c} \quad (36)$$

where

$$\mathbf{H} = \begin{bmatrix} \mathbf{s}_1 & \mathbf{s}_2 & \mathbf{s}_3 & \mathbf{s}_4 & \mathbf{s}_5 & \mathbf{s}_6 \\ \mathbf{q}_1 \times \mathbf{s}_1 & \mathbf{q}_2 \times \mathbf{s}_2 & \mathbf{q}_3 \times \mathbf{s}_3 & \mathbf{q}_4 \times \mathbf{s}_4 & \mathbf{q}_5 \times \mathbf{s}_5 & \mathbf{q}_6 \times \mathbf{s}_6 \end{bmatrix}$$

$$\mathbf{x} = [x_1 \, x_2 \, x_3 \, x_4 \, x_5 \, x_6]^{\text{T}}$$

$$\mathbf{c} = \begin{bmatrix} \Re\mathbf{F}_{\text{ext}} + M(\mathbf{g} - \mathbf{a}) - \sum_{i=1}^{6} \mathbf{K}_i \\ M\mathbf{R} \times (\mathbf{g} - \mathbf{a}) - \mathbf{I}\boldsymbol{\alpha} - \boldsymbol{\omega} \times \mathbf{I}\boldsymbol{\omega} + \Re\mathbf{M}_{\text{ext}} - \sum_{i=1}^{6}[\mathbf{q}_i \times \mathbf{K}_i - \mathbf{f}_i] \end{bmatrix}.$$

The linear system (36) can be solved for $\mathbf{x}$, and the required input forces can be determined from the vector (six dimensional) form of Equation (24) as

$$\mathbf{F} = \mathbf{D} - \mathbf{x} \quad (37)$$

where $\mathbf{F} = [F_1 \, F_2 \, F_3 \, F_4 \, F_5 \, F_6]^{\text{T}}$ and $\mathbf{D} = [D_1 \, D_2 \, D_3 \, D_4 \, D_5 \, D_6]^{\text{T}}$.

3.3 Solution for the constraint forces

For the purpose of control of the manipulator, the determination of the actuation forces in the legs is sufficient, as given by Equation (37). However, for the mechanical design, the constraint forces are also important. After $\mathbf{x}$ is known, the equations for the legs are decoupled and the forces in different legs can be determined separately. Equations (21), (26), (28), (27), (29) and (17) for each leg can be used to determine the joint reactions in the respective leg.

4. IMPLEMENTATION OF THE FORMULATION

The algorithm for the inverse dynamics of the Stewart platform described in the foregoing has been implemented in a program written in MATLAB. The equations are used in terms of vectors and matrices as they appear in the above sections and, as such, no effort has been made to minimize the computation.

The program has been developed to plan straight-line paths and compute the actuator forces to track them. It determines and plots the time histories of the six leg forces required to track the planned trajectories. The salient features of the implementation are discussed below.

4.1 Representation of orientation

The orientation of the platform with respect to the base has been represented by Roll–Pitch–Yaw angles as

$$\Re = \text{RPY}(\theta_z, \theta_y, \theta_x) = \text{Rot}(Z, \theta_z)\text{Rot}(Y, \theta_y)\text{Rot}(X, \theta_x). \quad (38)$$

4.2 Singularity and condition number

The computation of the actuator forces involves the solution of Equation (36) which is a system of six linear equations in six unknowns. If the coefficient matrix **H** turns out to be singular, the system may not have a solution. Physically, in such a situation, the manipulator is in a singular configuration gaining one or more degrees of freedom and no system of leg forces will be able to support the platform against the force system at the platform. Even when the matrix **H** is not exactly singular, but ill-conditioned (near a singularity), large leg forces may be needed to support the platform.

The proximity of a matrix to singularity is measured by the condition number of the matrix. The definition of the condition number used in the present work is the ratio of the greatest to least singular values of the matrix, where the singular values of a matrix **H** are the diagonal terms of the diagonal matrix Σ in the singular value decomposition (see page 203 of [8])

$$\mathbf{H} = \mathbf{U}\Sigma\mathbf{V}^{\mathrm{T}}$$

where both **U** and **V** are orthogonal for a square matrix **H**. Further, the singular values are the square-roots of the eigenvalues of $\mathbf{H}\mathbf{H}^{\mathrm{T}}$.

The condition number of the matrix **H** is ∞, when it is singular. In the best possible configuration, where the transformation is isotropic, the condition number is unity (all the singular values are equal).

As the matrix **H** has three dimensionless rows and the other three with linear dimensions, the condition number suffers from a theoretical disadvantage of being a ratio of two quantities of different dimensions. As such, in general, it is not possible to derive a condition number which is a true representative of the behaviour of the transformation associated with the matrix. However, in practical circumstances, it is possible to compare quantities of different dimensions through consideration of commonly encountered orders of magnitudes for the quantities. In the present case, the matrix **H** transforms six forces to three forces and three moments. The orders of magnitudes of the forces and the moments which are comparable depend on the kinematic parameters of the manipulator, essentially those parameters which enter the three last rows of **H**. Therefore, in the present situation, the condition number does give a reliable qualitative measure of the conditioning of the transformation.

4.3 Trajectory

For the implementation of the algorithm, straight line paths have been planned in Cartesian space. The orientation also has been planned by linear interpolation of the Roll–Pitch–Yaw angles. As functions of time, each coordinate (t_x, t_y, t_z, θ_x, θ_y and θ_z) is linear with parabolic blends at the beginning and the end, i.e. they change in three steps with constant acceleration, constant velocity and constant deceleration.

Initial and final configurations are taken in the form of $[\mathbf{t}_0, \boldsymbol{\theta}_0]$ and $[\mathbf{t}_1, \boldsymbol{\theta}_1]$. The total time interval τ_{f} and the magnitudes of maximum linear and angular velocities V and Ω are taken as inputs. The time interval τ_{t} for constant acceleration and deceleration in **t** is determined from

$$\tau_{\mathrm{t}} = \tau_{\mathrm{f}} - \frac{\|\mathbf{t}_1 - \mathbf{t}_0\|}{V} \tag{39}$$

and the value of the constant acceleration is

$$\mathbf{a}_{\mathrm{t}} = \frac{V}{\tau_{\mathrm{t}}} \frac{\mathbf{t}_1 - \mathbf{t}_0}{\|\mathbf{t}_1 - \mathbf{t}_0\|}. \tag{40}$$

For orientation, similar expressions for the time interval τ_{θ} for constant angular acceleration and deceleration, and the value of the constant angular acceleration $\mathbf{a}_{\theta}$ are obtained. With these parameters, the trajectory planned for each of the six coordinates has a typical shape as shown in Fig. 3.

The trajectory planning scheme described above has been selected just for simplicity. In fact, any scheme for planning the trajectory in the Cartesian space can be used with equal ease with the present dynamic formulation. If the trajectory is planned in joint space, the forward kin-
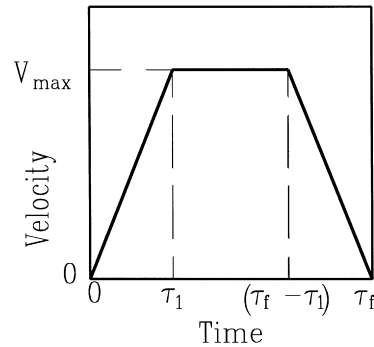
Fig. 3. Typical trajectory for each coordinate.

ematics for position, velocity and acceleration has to be solved at each time-step. This basically involves the solution of a non-linear system of six equations represented by Equation (2)† for position and two linear systems represented by Equations (5) and (8) for velocity and acceleration, respectively. This makes the joint–space trajectory planning computationally more expensive and hence, less attractive, which is a common feature of parallel manipulators.

4.4 Static and dynamic forces in legs

If the dynamic and gravity effects of the legs and the viscous friction at the joints are neglected, we obtain $\mathbf{C} = 0$ in Equation (20), hence $\mathbf{K} = 0$ in Equation (21). Also, $\mathbf{D} = 0$ in Equation (37) and $\mathbf{f}_i = 0$.

Consequently, $\mathbf{F}_0 = -\mathbf{x}_0$ and $\mathbf{H}\mathbf{x}_0 = \mathbf{c}_0$, where

$$\mathbf{c}_0 = \begin{bmatrix} \Re\mathbf{F}_{ext} + M(\mathbf{g} - \mathbf{a}) \\ M\mathbf{R} \times (\mathbf{g} - \mathbf{a}) - \mathbf{I}\boldsymbol{\alpha} - \boldsymbol{\omega} \times \mathbf{I}\boldsymbol{\omega} + \Re\mathbf{M}_{ext} \end{bmatrix}.$$

Hence, the leg forces $\mathbf{F}_0$ due to constraints only are given by

$$\mathbf{H}\mathbf{F}_0 = -\mathbf{c}_0 \tag{41}$$

and the difference

$$\mathbf{F}_d = \mathbf{F} - \mathbf{F}_0 \tag{42}$$

stands for the part of the actuator forces accounting for the leg inertia and the joint friction.

The actuator forces $\mathbf{F}$ in the legs, the constraint forces $\mathbf{F}_0$ obtained from static force transformation (which incorporates the inertia of the platform, but does not include leg inertia) and the difference $\mathbf{F}_d$ are plotted on the same scale along the trajectory as functions of time to justify the complete dynamic formulation and to visualise the difference made by considering the simplistic assumption of massless legs and frictionless joints. An additional set of plots shows the fraction of the dynamic forces $\mathbf{F}_d$ to the total forces $\mathbf{F}$. This fraction, namely F_d/F, for the various legs will be referred to hereafter as "fraction of dynamic forces" or simply "dynamic fraction". The condition number of the manipulator also has been plotted along the trajectory to examine the nature of the forces with reference to the geometric configuration of the manipulator.

4.5 Computational complexity

In order to assess the suitability of the formulation for real-time control, a measure of the computational load is useful. To get this information, the MATLAB function "flops" has been used at a few significant locations in the program and the numbers of floating point operations required at various segments of the program have been obtained. For each time-step, the numbers of floating point operations in different parts of the algorithm as obtained from the MATLAB function "flops" are as follows.

---

†Six equations are obtained from six legs.

Computation for each leg (Section 2): 694 floating point operations.
Computation involving platform only: 273 floating point operations.
Final system of equations: 452 floating point operations.

Thus, the total number of floating point operations is 4889. At this point, it is interesting to compare this computational load with the corresponding data for the Newton–Euler formulation for a 6-dof serial manipulator.

Fu et al.[9] give the numbers of multiplications and additions for the Newton–Euler approach for the inverse dynamics of a n-dof serial manipulator as $132n$ and $111n - 4$, respectively (see page 132 of[9]), a total of 1454 floating point operations for a 6-dof serial manipulator. Thus, the computational load for the present formulation for the Stewart platform is only 3.36 times that of a 6-dof serial manipulator. This economy of computation for such a complicated manipulating structure like the Stewart platform seems to be quite remarkable.

Moreover, it is to be noted that the formulation possesses an inherent parallelism. The computations for each leg (694 flops) and those involving platform only (273 flops) are completely decoupled and there is no data dependency among these seven (six for legs and one for platform) branches of computations. So, if implemented in a parallel-processing environment, the algorithm will have little parallelising overhead and the computational time needed is expected to be of the same order as that of the Newton–Euler formulation for a serial manipulator.

For the above estimate, calculations needed for the actuating forces only have been considered. Apart from that, in order to compare with the corresponding data available in literature regarding computational requirement for the serial manipulators, the calculations required for the viscous friction terms have not been counted.

5. RESULTS AND DISCUSSION

The program described above has been used with a Stewart platform manipulator, the description of which is given in the Appendix. The test manipulator has its kinematic and dynamic parameters quite arbitrary in the sense that no symmetry assumption has been made in the selection of the connection-points in the base and in the platform. Again, the parts of the leg have been taken with asymmetric distribution of inertia. The relative values of the parameters have been kept realistic and identical dynamic parameters have been taken for all legs, i.e. the lower parts of all the six legs are identical and the upper parts of the six legs are identical, though this is not mandatory for the algorithm. No limitation has been imposed on the leg lengths for the implementation of the program and it is assumed that the leg lengths assumed by the legs during the tracking of the test trajectories are within limits and the whole trajectory falls within the workspace of the manipulator. In the case of an actual manipulator, there will be well-defined limits on these lengths, which have to be satisfied at the task development and path planning stage. The external force $\mathbf{F}_{ext}$ and moment $\mathbf{M}_{ext}$ have been taken as zero for all the tasks studied below. However, the program incorporates external forces and moments also and, if the force feedback data are available, they are automatically handled by the program. The results of the computation with a few straight-line paths are described below.

5.1 Normal well-conditioned paths

Path I. The parameters of the path are as follows. Here, and in subsequent examples, SI units (m, kg, s, rad) have been used for all quantities.

$$\mathbf{t}_0 = [0.1\ 0.0\ 0.4]^t, \quad \theta_0 = [0.0\ 0.0\ -0.2]^T$$

$$\mathbf{t}_1 = [0.3\ 0.0\ 0.6]^T, \quad \theta_1 = [0.0\ 0.0\ 0.2]^T$$

$$\tau_f = 6, \quad V = 0.08, \quad \Omega = 0.08, \quad d\tau = 0.1.$$

The plots of actuator forces required in the six legs to track this trajectory are shown in Fig. 4. The total forces $\mathbf{F}$, the forces $\mathbf{F}_0$ (obtained by taking massless legs and frictionless joints) and the difference $\mathbf{F}_d$ are shown by different line-styles and are indicated by letters " T", " S" and "D", respectively. It is seen that the leg forces are moderate (of the same order as the weight of the platform and payload, which has been taken as 40 kg) and vary smoothly along the trajec-
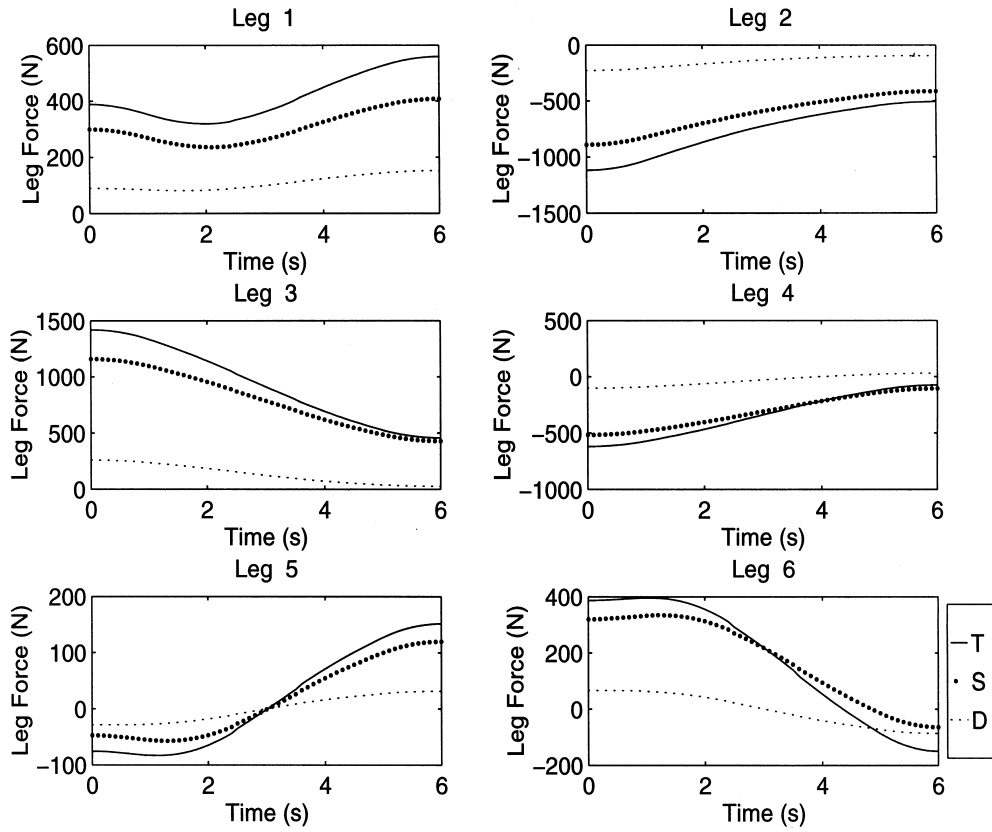
Fig. 4. Path I—leg forces.

tory. This is a consequence of the manipulator being quite well-conditioned (far from singularity) for this trajectory, as is evident from the plot of the condition number of the matrix **H** along the trajectory (see Fig. 5).

The plots of dynamic fractions of forces, as shown in Fig. 6, show that the leg inertia contributing around 20% of the force demand at the actuators is quite common and the maximum may even go up to 40%. (The sudden jump sign in the dynamic fractions in legs 5 and 6 is not much significant, because near that instant the total force for that leg crosses zero.) This information clearly identifies the necessity to consider the leg inertia in the dynamic formulation of the Stewart platform. In this example, each leg is of mass 4 kg. Hence, with a platform (and payload) mass of 40 kg, the platform to leg mass ratio is 10. With this realistic mass ratio†, the leg inertia is found to be significant. The contribution of the leg inertia is much more pronounced when the platform and payload mass is less. If the platform mass is taken to be of the same order as the mass of a leg, this dynamic fraction is often found to be above 60% (those plots are not presented due to lack of space).

Path II. The second trajectory discussed essentially follows the same path as the first, but with a higher speed (10 times). So, among the trajectory parameters, $\mathbf{t}_0$, θ_0, $\mathbf{t}_1$ and θ_1 remain the same while the other parameters have values as follows.

$$\tau_f = 0.6, \quad V = 0.8, \quad \Omega = 0.8, \quad d\tau = 0.01.$$

The plots shown in Figs 7 and 8 indicate that this difference in speed results in significant rise in the bounds of the leg forces and the dynamic fractions and their distribution is also altered significantly. The steep change in the leg forces at a few instants is basically the result of similar steep changes in the leg accelerations at those instants. This shows that at such high speeds, the

---

†It is to be remembered that the use of parallel manipulator is mostly in situations where high load capacity is important.
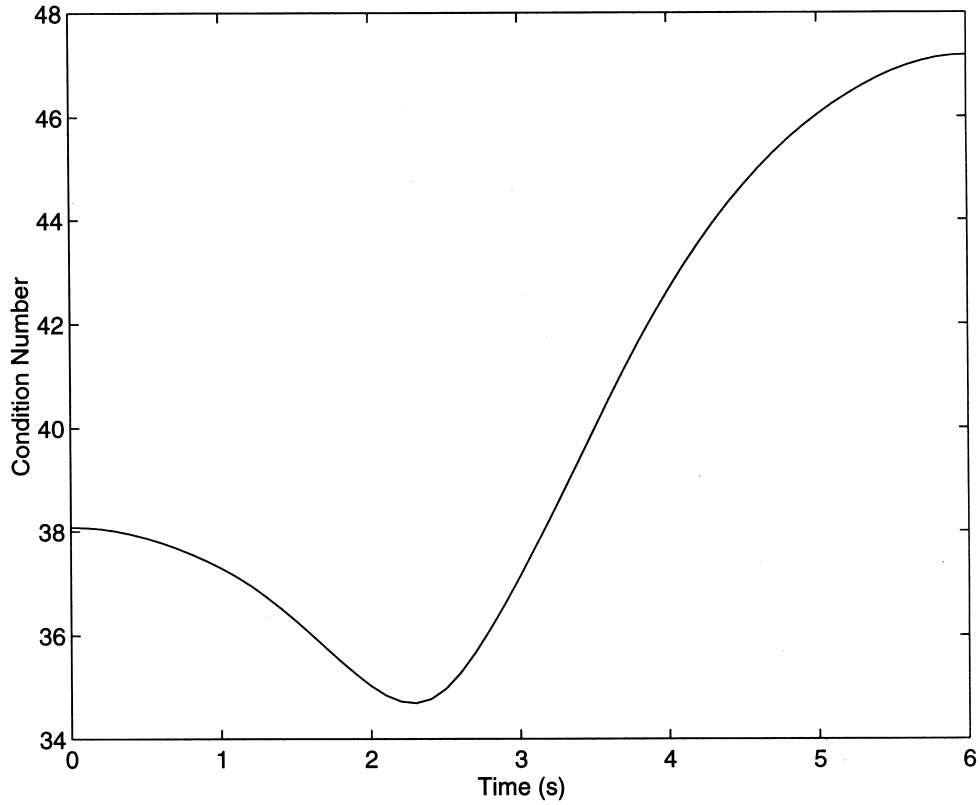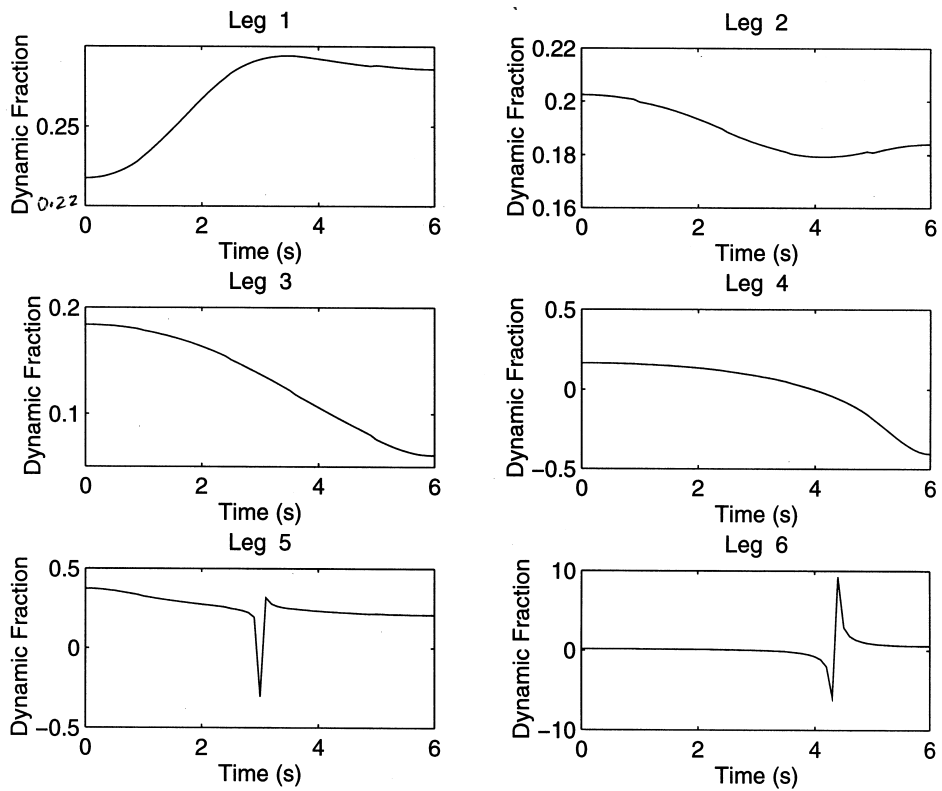
Fig. 5. Path I—condition number.

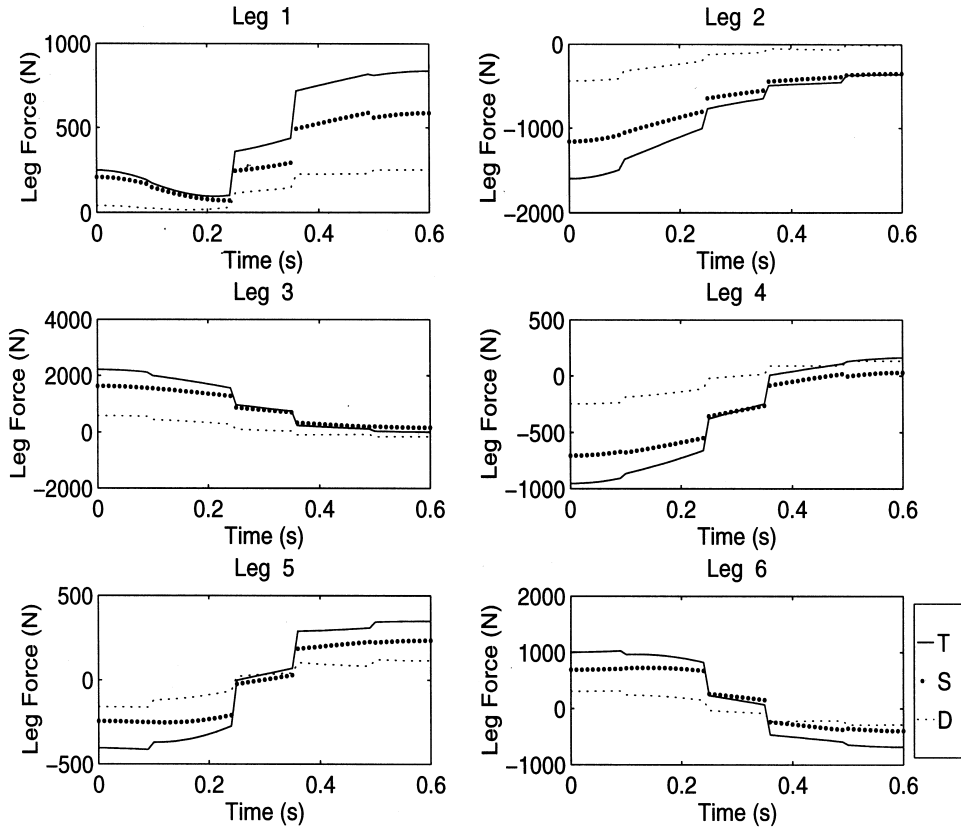Fig. 6. Path I—fraction of dynamic forces.
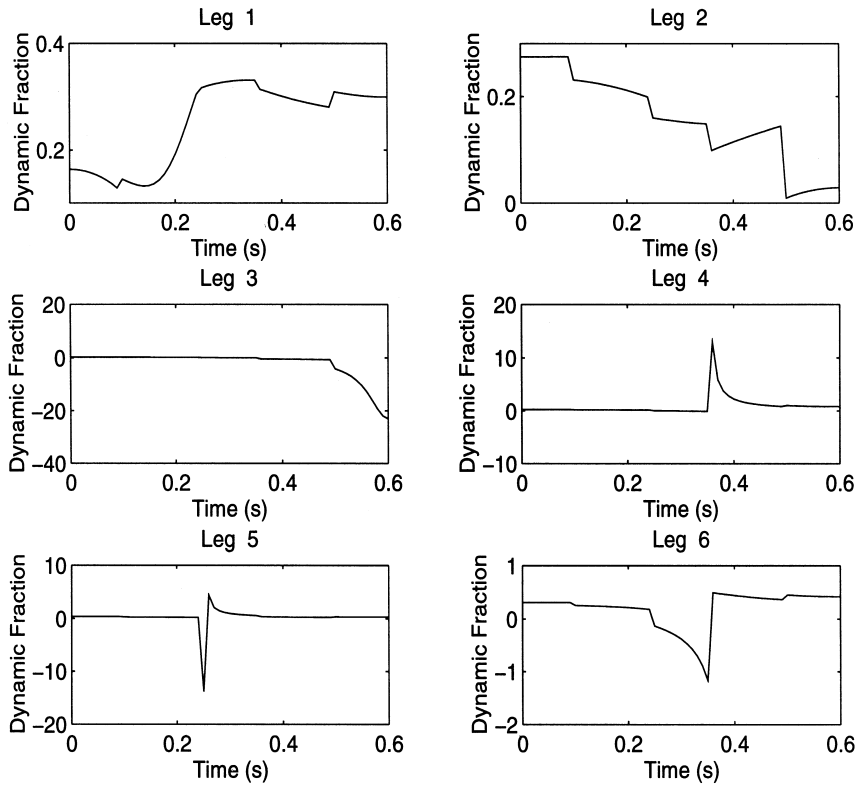
Fig. 7. Path II—leg forces.

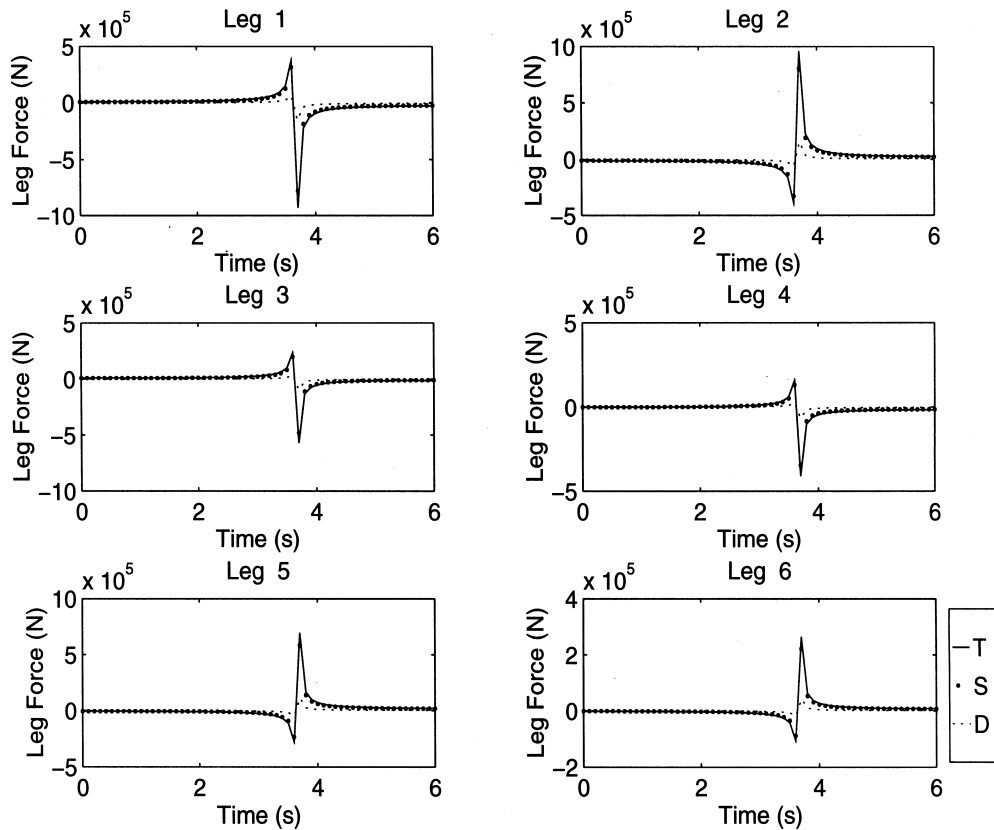Fig. 8. Path II—fraction of dynamic forces.

Fig. 9. Path III—leg forces.

dynamic effects of the whole manipulator have an important bearing on the required actuator forces.

5.2 Singular and ill-conditioned paths

It is expected that trajectories which pass through singularities may demand infinite magnitude of forces at the actuators and hence may not be practicable. Following is the study of such a path.

Path III. The parameters of the path under discussion are as follows:

$$\mathbf{t}_0 = [0.4 \ 1.4 \ 1.2]^T, \quad \theta_0 = [0.1 \ 0.2 \ 0.0]^T$$

$$\mathbf{t}_1 = [0.8 \ 1.8 \ 1.8]^T, \quad \theta_1 = [0.3 \ 0.4 \ 0.0]^T$$

$$\tau_f = 6, \quad V = 0.2, \quad \Omega = 0.08, \quad d\tau = 0.1.$$

The plots of leg forces for this path (Fig. 9) show a clear singularity where suddenly the force requirements at the actuators are very high (of the order of 10^5 N). This singularity can be predicted from the plot of condition number (Fig. 10), in which precisely at that location of the trajectory the condition number is seen to have a sharp rise. Obviously, such high magnitudes of forces cannot be supplied by the actuators. Consequently, the legs fail to support the platform and it tends to wander under even a small external load or due to the gravity or inertia of the platform.

Other cases studied, but not reported here, indicate that even for a trajectory which does not actually encounter a singularity, but is near to one, the near-singular or ill-conditioned behaviour being detected by the high condition number (say, of the order of 10^2 or 10^3), the force requirements at the actuators are quite high (say, of the order of 10^4 N or more). In such cases also, the actuators may fail to sustain the load at the end-effector (platform) and the manipulator may lose rigidity to some extent.
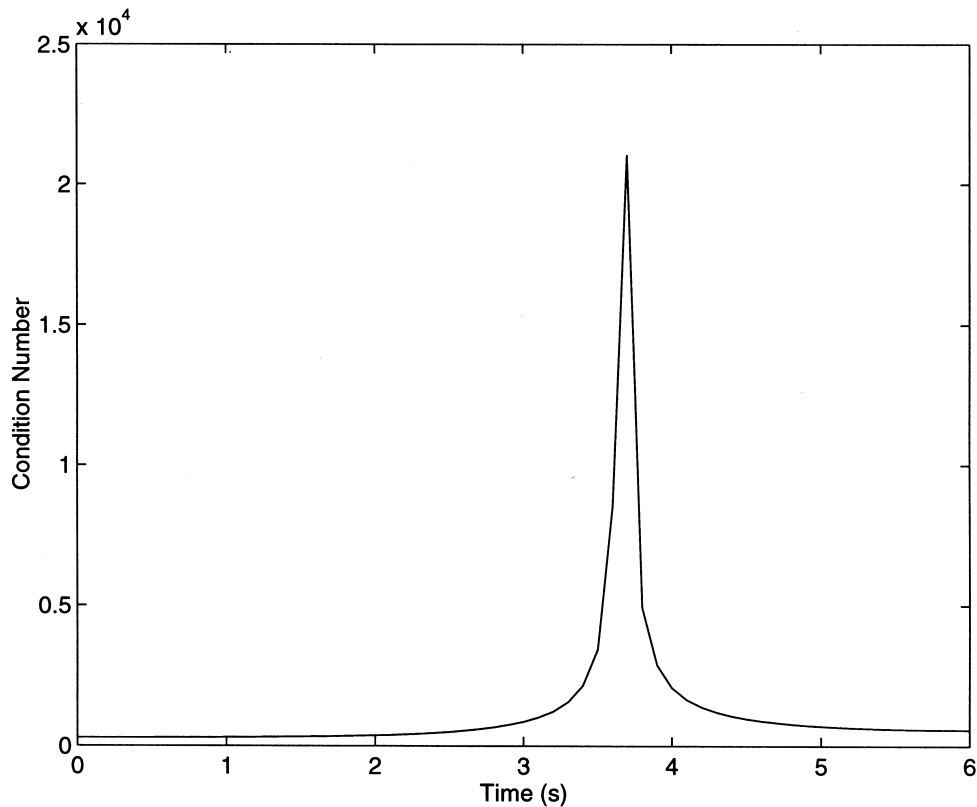
Fig. 10. Path III—condition number.

6. CONCLUSIONS

The inverse dynamics problem of the Stewart platform manipulator has been formulated by the Newton–Euler approach and an algorithm has been developed to compute the actuator forces in the legs to track given trajectories. All the unknowns pertaining to one leg have been expressed in terms of one unknown by eliminating others. Finally, these six unknowns for the six legs have been solved from the dynamic equations of the platform and the actuator forces are computed. The joint reactions also can be calculated with a small amount of additional computation.

This formulation for the inverse dynamics of the Stewart platform incorporates all the dynamic effects and is computationally efficient. A comparison with the corresponding data for serial manipulators shows that the number of floating point operations for the algorithm presented here is just about 3.36 times that of a 6-dof serial manipulator. Moreover, the inherent parallelism of the manipulator itself and that of the formulation can be utilized in a parallel computing environment to make the computational time even less than that for a 6-dof serial manipulator.

The algorithm has been implemented in a MATLAB program and a few trajectories have been studied for a test manipulator. The results show that the consideration of the leg inertia is quite important for the dynamics of the Stewart platform manipulator, because it has been generally found to contribute 20–50% of the forces demanded at the actuators. This fraction of force is found to increase when the speed is high and the payload is less.

The simulation results further show that there is a direct relation between the required actuator forces and the condition number of the manipulator. For a given Stewart platform manipulator, higher the condition number, higher are the actuator forces. Hence, the importance of a path-planning scheme minimizing the condition number along the whole path is quite apparent. The present work focuses the attention on the need for such an optimal path-planning scheme.

The scope for future work includes the development of closed form dynamic equations of the Stewart platform based on this formulation which will be useful for the purpose of simulation and the design of control systems.

REFERENCES

1. Stewart, D., A platform with six degrees-of-freedom, in *Proceedings of the Institute of Mechanical Engineers Part I,* Vol. 180, 1965–1966, pp. 371–386.
2. Merlet, J. P., *Parallel manipulators Part I: theory. Design, kinematics, dynamics and control*, INRIA Report, 1987.
3. Fichter, E. F., *International Journal of Robotic Research*, 1986, **5**(2), 157–182.
4. Do, W. Q. D. and Yang, D. C. H., *Journal of Robotic Systems*, 1988, **5**(3), 209–227.
5. Geng, Z., Haynes, L. S., Lee, J. D. and Carroll, R. L., *Robotics and Autonomous Systems*, 1992, **9,** 237–254.
6. Liu, K., Fitzgerald, M., Dawson, D. W. and Lewis, F. L., Modelling and control of a Stewart platform manipulator, ASME DSC Vol. 33, *Control of Systems with Inexact Dynamic Models*, 1991, pp. 83–89.
7. Ji, Z., Study of the effect of leg inertia in Stewart platforms, in *Proceedings of the IEEE International Conference of Robotics and Automation,* Vol. 1, 1993, pp. 121–126.
8. Forsythe, G. E., Malcolm, M. A. and Moler, C. B., *Computer Methods for Mathematical Computations*, Prentice-Hall Inc., New Jersey, 1977.
9. Fu, K. S., Gonzalez, R. C. and Lee, C. S. G., *Robotics: Control, Sensing, Vision and Intelligence*, McGraw-Hill, New York, 1987.

APPENDIX

Description Of The Test Manipulator

The Stewart platform used as the test manipulator for the simulation studies in Section 5 has the following kinematic and dynamic parameters (all in SI units).

Base points:

$$[\mathbf{b}_1\ \mathbf{b}_2\ \mathbf{b}_3\ \mathbf{b}_4\ \mathbf{b}_5\ \mathbf{b}_6] = \begin{bmatrix} 0.6 & 0.1 & -0.3 & -0.3 & 0.20 & 0.5 \\ 0.2 & 0.5 & 0.3 & -0.4 & -0.30 & -0.2 \\ 0.0 & 0.1 & 0.1 & 0.0 & -0.05 & 0.0 \end{bmatrix}.$$

Unit vectors along fixed axes of universal joints:

$$[\mathbf{k}_1\ \mathbf{k}_2\ \mathbf{k}_3\ \mathbf{k}_4\ \mathbf{k}_5\ \mathbf{k}_6] = \begin{bmatrix} -0.8141 & 0.2308 & 0.9535 & 1.0000 & 0.7071 & -0.9535 \\ 0.2714 & 0.9231 & 0.2860 & 0.0000 & 0.7071 & 0.2860 \\ 0.0000 & 0.3077 & 0.0953 & 0.0000 & 0.0000 & -0.0953 \end{bmatrix}.$$

Platform points (in platform frame):

$$[\mathbf{p}_1\ \mathbf{p}_2\ \mathbf{p}_3\ \mathbf{p}_4\ \mathbf{p}_5\ \mathbf{p}_6] = \begin{bmatrix} 0.3 & 0.3 & 0.0 & -0.2 & -0.15 & 0.15 \\ 0.0 & 0.2 & 0.3 & 0.1 & -0.20 & -0.15 \\ 0.1 & 0.0 & 0.0 & -0.1 & -0.05 & -0.05 \end{bmatrix}.$$

Mass of lower and upper part of each leg:

$$m_{\mathrm{d}} = 3.0 \quad \text{and} \quad m_{\mathrm{u}} = 1.0.$$

Centres of gravity of lower and upper parts of each leg (in local frames):

$$\mathbf{r}_{\mathrm{d}_0} = [0.4\ 0.14\ -0.18]^{\mathrm{T}} \quad \text{and} \quad \mathbf{r}_{\mathrm{u}_0} = [-0.6\ -0.08\ 0.08]^{\mathrm{T}}.$$

Moments of inertia of lower and upper parts of each leg (in local frames):

$$\mathbf{I}_{\mathrm{d}_0} = \begin{bmatrix} 0.010 & 0.005 & 0.007 \\ 0.005 & 0.002 & 0.003 \\ 0.007 & 0.003 & 0.001 \end{bmatrix} \quad \text{and} \quad \mathbf{I}_{\mathrm{d}_0} = \begin{bmatrix} 0.005 & 0.002 & 0.002 \\ 0.002 & 0.002 & 0.001 \\ 0.002 & 0.001 & 0.003 \end{bmatrix}.$$

Platform mass (including payload):

$$M = 40.0.$$

Centre of gravity of the platform and payload (in platform frame):

$$\mathbf{R}_0 = [0.04\ 0.03\ -0.06]^{\mathrm{T}}.$$

Moment of inertia of platform and payload (in platform frame):

$$\mathbf{I}_{\mathrm{p}} = \begin{bmatrix} 0.050 & 0.003 & 0.004 \\ 0.003 & 0.040 & 0.003 \\ 0.004 & 0.003 & 0.100 \end{bmatrix}.$$

Coefficients of viscous friction:

$$C_{\mathrm{u}} = 0.0001$$
$$C_{\mathrm{p}} = 0.001$$
$$C_{\mathrm{s}} = 0.0002.$$